# Grid Code Enablement and C-HIL Validation of Distributed Energy Resources with OpenFMB

Rasik Sarup[1], Joshua Hambrick[1], Cory Brown[1], Idrissa Agalassou Alassane[1], Michael Burck[1], Dwayne Bradley[2], Fares Al Jajeh[3], Émile Grégoire[3], Charles Fallaha[3], Sayani Seal[3], Faisal Mumtaz[3], Stuart Laval[4]
[1]*Open Energy Solutions Inc., USA*
[2]*Duke Energy, USA*
[3]*Eaton Corporation, Canada*
[4]*Eaton Corporation, USA*
Idrissa@openenergysolutionsinc.com
Dwayne.Bradley@duke-energy.com
FaresAlJajeh@eaton.com

***Abstract*—Distributed Energy Resources (DERs) with grid support capabilities enabled by IEEE 1547-2018 must be designed and evaluated in a systematic and comprehensive way. These capabilities, which are often referred to as grid codes, surpass the base capabilities of a DER and provide opportunities to improve grid reliability through increased resiliency to disturbances, proper active-reactive response, and operational visibility. This paper introduces a methodology to add grid code functionality to legacy DERs with an OpenFMB communication framework with the ultimate objective of enabling grid support functions using Distributed Intelligence (DI). Additionally, the content below provides a framework for validating the impact of these devices using a state-of-the-art Controller Hardware in Loop (C-HIL) testbed.**

***Keywords— Grid codes, C-HIL, OpenFMB, 1547, DER, distributed intelligence***

## I. Introduction

With the increasing penetration of DERs, passive participation in the grid can put the bulk power system at risk due to frequent tripping [1]. An opportunity loss is also present as DERs can provide voltage and frequency support. Furthermore, the dominant DER technology has shifted from rotating machines to Inverter Based Resources (IBR) [2]. These IBR have different operating characteristics and capabilities as compared to rotating machines which can have significant impact on both the local distribution system where they are connected, as well as, in aggregate, on the bulk power system. For this reason, interconnection standards such as IEEE 1547 have been revised to define a new set of allowable and required behavior for DERs [3].

Another challenge is the interoperability and DERs integration from an information technology standpoint [1], [4]. Towards this end, the usage of a distributed message bus to publish configurations and subscribe to events has grown a lot of interest. One such innovation is Open Field Message Bus (OpenFMB) [5], [4]. In early 2016, OpenFMB became a ratified standard from the North American Energy Standards Board (NAESB) as a framework for grid-edge interoperability of electric grid device and application. This standard trades the legacy approach of polling devices for data and instead uses publish/subscribe patterns to efficiently share data in a more peer-to-peer approach. It also defines the process of how device and application data models should be established.

The first evolution of OpenFMB was demonstrated at DistribuTECH 2016 among multiple vendor booths live on the exhibit hall floor. This demonstration gave an awareness of the power of using publish/subscribe and common device data models to show how interoperability could be a huge benefit for the industry. After an update to the NAESB standard in 2020 to allow for more rapid evolutions of the data models, OpenFMB v2.0 of the data model was released to incorporate both IEC Common Information Model (CIM) and IEC 61850 logical node data structures [6], [7]. Currently, the OpenFMB v2.1 data model is leveraging artifacts from IEC 61850-7-420 in order to add and realize the grid code definitions from IEEE 1547-2018 for energy storage devices, solar inverters and generation devices to further enhance interoperability.

This paper introduces a methodology to integrate grid code functionality to legacy DERs using OpenFMB as a communication framework. A solar photovoltaic (PV) inverter and a battery energy storage system (BESS) are used as two legacy DER modules. A modular programmable logic controller (PLC) based controller, is used to provide inverter control as per IEEE 1547-2018 based grid code functionalities. A validation of the methodology is presented using a C-HIL testbed.

## II. Grid Code Controller

### *A. Grid Code Implementation*

Grid codes refer to a collection of DER capabilities and requirements that are intended to support the safe and reliable operation of the grid with high DER penetrations. While grid codes may be defined differently across various relevant interconnection standards in general, grid codes refer to active power and frequency support, reactive power and voltage support, ride-through requirements (voltage and frequency) as well as some protection requirements (e.g., anti-islanding).

The grid code controller presented has a complete implementation of IEEE 1547-2018 and was validated according to the IEEE 1547.1 testing standard. However, since there are many grid-code functions that could be elaborated on, the paper is focused mainly on the following four functions:

- Enter service
- Voltage-reactive power (Volt-VAR)
- Frequency-droop and active power (Hz-Watt)
- Voltage trip including cease to energize

## *B. Data Model and OpenFMB*

Distributed intelligence (DI) allows for effective integration of dissimilar hardware and gives equal access to software vendors by making distribution level decisions in real time. DI provides seamless interaction as desired by the application provider or the asset owners and operators. To enable DI, OpenFMB v2.1 was implemented in the grid code controller, which includes grid codes data structures for energy storage systems and solar inverters that are leveraged in this paper to showcase interoperability and distributed intelligence. The data model is closely based on IEEE Std 1547-2018. Fig. 1 shows the communication diagram. The colored lines are all using OpenFMB messages.

For this setup, an OpenFMB adapter was configured to read measurement values from the BESS communicating with Modbus protocol and publishing the values as OpenFMB messages to a NATS publish-subscribe message broker running in the laboratory. It also subscribed to that broker to convert OpenFMB messages containing active and reactive power setpoints to the device. Similarly, another adapter was configured to perform the same tasks but for the simulated PV inverter, emulated in Typhoon HIL [8], using Distributed Network Protocol 3 (DNP3). There is also a DNP3 adapter in front of the BESS transformer protection relay, SEL-487E, which subscribed to enter service and trip commands.

With all these adapters in place, the Grid Code Controller only interacted with the external devices using the OpenFMB data model. The specificity of protocol translation is decoupled from the control algorithms, so the protocol adapters and the Grid Code Controller were running on the same hardware, but they could easily be distributed across low-cost controllers, and could be modularized for various use cases.

The Grid Code Controller received new configuration parameters (known as Management Information in IEEE Std 1547-2018, section 10.6 [3]) through the OpenFMB model. This information was embedded inside a schedule to allow an electric utility System Operator to program the DER for the current objective at regular intervals. Fig. 2 presents the Unified Modeling Language (UML) diagram of the data model for the grid codes section of the energy storage system with the relevant Management Information highlighted. In this setup, the schedule was configured using a simplistic Human-Machine Interface (HMI) on a laptop and sent to the centralized NATS broker. The HMI also received the measurements published by the protocol adapters through the NATS broker and displayed the value to the operator.

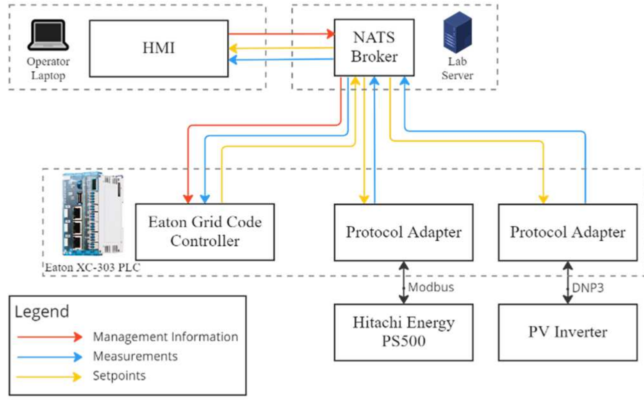


Fig. 1 Communication diagram

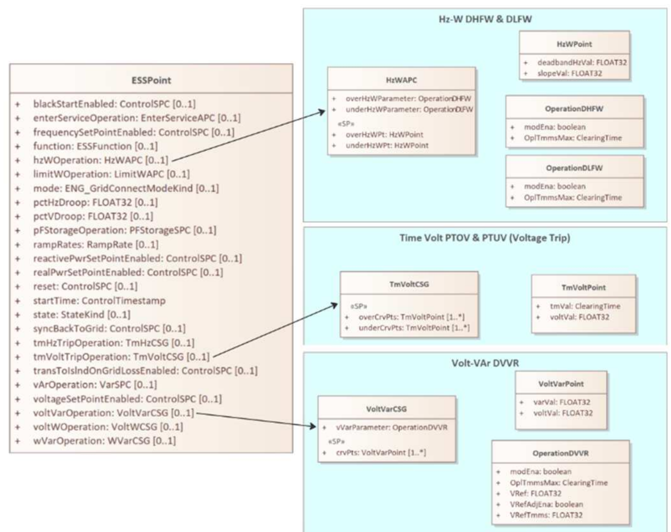


Fig. 2 UML diagram

## TESTBED OVERVIEW

## *C. Background*

The testbed, built by Duke Energy in collaboration with Open Energy Solutions Inc. at Mt. Holly Microgrid Test facility, leverages a C-HIL simulator combined with a reference Information Technology / Operations Technology (IT/OT) implementation of Open Field Message Bus (OpenFMB). The testbed can evaluate DER conforming to the latest IEEE 1547.1 based interconnection requirements. This architecture provides detailed insight (readings, controls, statuses) on every grid-edge node which increases situational awareness and reduces the burden of interconnection of DER for purposes of testing with the existing grid assets.

Hardware-in-loop (HIL) is a platform that enables Intelligent Electronic Devices (IEDs) to integrate with the software interface that can facilitate the incoming digital and analog signals creating a digital twin of the actual system. This architecture can be subcategorized into Controller Hardware in Loop (C-HIL) [9] which utilizes the brain of the equipment, i.e., controller of the IED; for example: recloser controller, voltage regulator controller, breaker controller, etc. Controller hardware in loop (C-HIL) is best characterized by [10] as a “nondestructive” way of testing IEDs with less risk to equipment and safety. This platform provides flexibility to utilize physical device controllers, simulated models, and digital interfacing components and perform various tests in real time with high accuracy.

The digital twin lab provides a platform to tune the simulation model of the microgrid to the highest accuracy level as it utilizes the reference parameters from the actual Mt. Holly microgrid in real time. This architecture enables the verification of IEEE 1547.1 grid codes on Battery and PV inverter controllers using OpenFMB. Leveraging HIL provides flexibility to perform real-time testing of multiple grid codes including Volt-VAR, Volt-Watt and Hz-Watt in a laboratory environment.

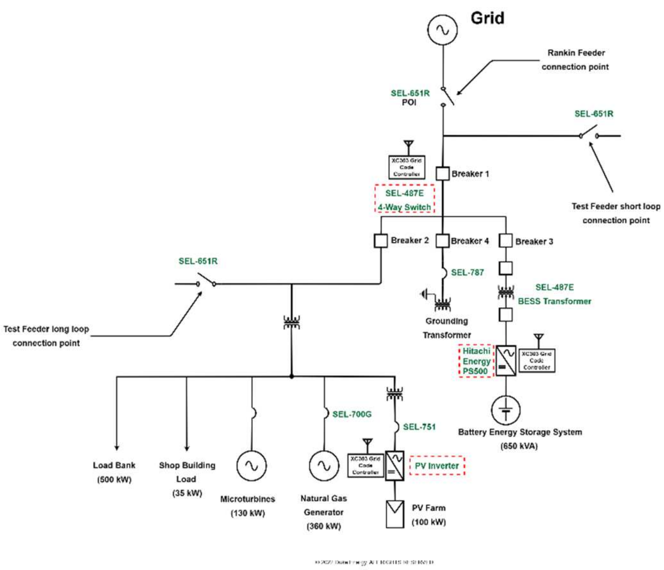


Fig. 3 Single line diagram of Mt. Holly microgrid indicating the OpenFMB nodes

The OpenFMB specification and its associated DI architecture are intended to support centralized, distributed analytics and control arrangements. This architecture not only provides access to local coordination and optimization but also supports general local connectivity and local peer-to-peer (publish and subscribe). In Fig. 3 OpenFMB Nodes are located at the antenna symbols (next to the red boxes) where there are adapters between OpenFMB and Modbus for the PS500 inverter [11] and DNP3 for simulated PV inverter as well as SEL-487E transformer protection relay.

### D. *Proposed Testbed*

The proposed C-HIL testbed demonstrated and enabled the distributed intelligence to federate the data at the grid edge by coordinating between the XC303 Grid Code Controller [12] and a BESS in real-time.

See Fig. 4 for integration methods. The BESS inverter controller, which was an Energy PowerStore500 (PS500), was integrated using Method 1. The PV inverter controller (simulated virtually in the HIL model) was configured using Method 2 with the proposed testbed. Both methods [13] allow for the Grid Code Controller to function as designed while demonstrating interoperability.

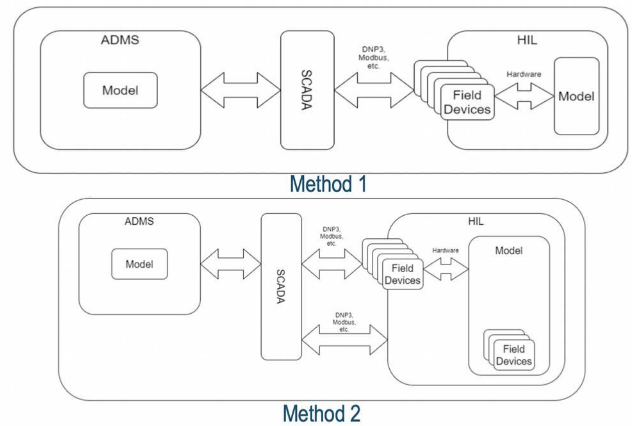


Fig. 4 Method 1 demonstrates the integration of PS500 with the HIL testbed and Method 2 demonstrates the integration of PV inverter with the testbed

The model under test comprises Duke Energy’s Rankin feeder (primary), Lumber Lane feeder (secondary), Mt. Holly Microgrid, and Test Feeder (under construction at the time) as shown in Fig. 3Fig. . The relay that provides protection and control to the 4-breaker switchgear at the Duke Mt. Holly Microgrid is an SEL-487E [14]. Breaker 1 of the switchgear is the point of common coupling that connects to a 12.47kV distribution feeder point of interconnection (POI). Additionally, breaker 1 provides a synchronism check by monitoring the deltas of voltage, frequency, and angle between the grid and the microgrid. The threshold of these deltas govern the mode of the Battery Energy Storage System (BESS) inverter: grid forming if the deltas are out of thresholds and grid following once the synchronism check is within the threshold. The integration setup of SEL-487 with the C-HIL testbed is shown in Fig. 5.

With this research/test, the functionality of the Grid Code Controller was verified by sending commands from two Eaton XC303 PLCs to the simulated PV inverter and the Hitachi Energy PowerStore PS500. The PS500 provided a flexible power electronics platform for battery energy storage systems integration. It was comprised of two EPC power controller cards and can detect islanding conditions, transitioning from grid following to grid forming mode. The BESS inverter only transitioned back to grid following mode after a synchronism check and a Modbus command sent from the XC303 Controller to the PS500. EPyQ software [15] was used as an interface for the PS500 and can be used to configure the inverter control by communicating with a computer through CAN and Modbus.

The PS500 was integrated with the C-HIL testbed at Duke Energy Mt. Holly and sent switching signals using the digital input per leg as shown in Fig. 6.

The digital inputs were configured within the HIL schematic editor and scaled to work with the amplifier with the specifications provided in TABLE I and TABLE II.

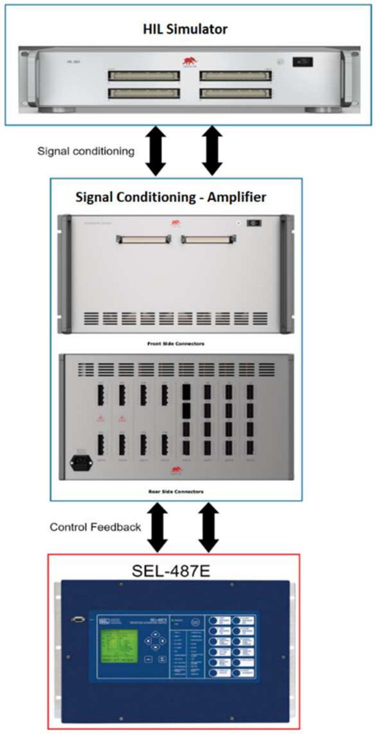


Fig. 5 Integration of SEL-487E with C-HIL Testbed

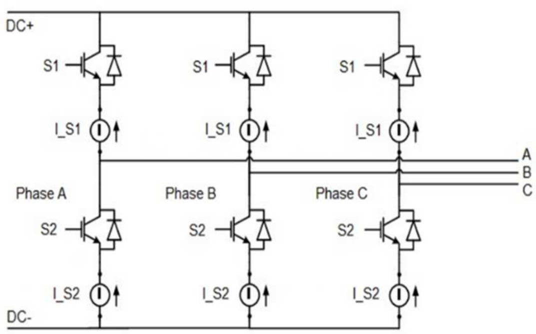


Fig. 6 Six-legged three phase – two level inverters

TABLE I. Three Phase Inverter Switches Settings

| | Digital Input # | Control Logic |
|---|---|---|
| **Phase A S1** | 32 | Active High |
| **Phase A S2** | 26 | Active High |
| **Phase B S1** | 31 | Active High |
| **Phase B S2** | 25 | Active High |
| **Phase C S1** | 30 | Active High |
| **Phase C S2** | 24 | Active High |

TABLE II. Digital Input Specification

| Type | Logic | Qty | Input resistance | Rating | Comment |
|---|---|---|---|---|---|
| Voltage | Fast-IO/ Potential | 32 | 100 kΩ/1.8 kΩ | Logic High: 2. 5.28 V Logic Low: 0..0.8 V | Default: Fast IO |

The analog readings were measured across the terminals of the equipment and amplified based on the specification provided in TABLE III.

TABLE III. Analog Output Specification

| Type | Range (peak) | Qty | Bandwidth | Accuracy | Comment |
|---|---|---|---|---|---|
| Analog Output | ±10V/ ±20 mA | 32 | DC-100 kHz | 0.1% + 500 µV 0.1% + 10 µA | Load range: > 500 < 500 |
| High Voltage | 183.3 V | 16 | DC-10 kHz | 1% + 10 mV | 1 mA output current |
| Current Output | 2.82 A | 16 | DC-120 kHz | 0.1% + 600 uA | 2 V compliance |

## III. Experimental Results

This section showcases the experimental results of the grid codes behavior implemented in each XC303 grid code controller for the BESS and the PV systems. Four test cases are presented based on the functions listed in Section II.A.

Case I showcases the 1547 Enter Service function on the BESS (Fig. 7). At time = 8 seconds the DER entered service as indicated by the Enter Service Flag as the voltage and frequency are within preset thresholds. The active power ramped up and reached the final steady value of 0.8 pu at time = 28 seconds as configured. The active power ramp rate was configured at 0.04 pu/s. Prior to the Enter Service function, the unit was acting as a grid forming unit with an active power delivery of 0.22 pu.

Case II is presented in Fig. 8 where the Volt-VAR grid code function was tested on the BESS. The expectation is that if the voltage increases the BESS should absorb reactive power per the Volt-VAR curve and should inject reactive power should the voltage decrease again. To test the function, an overvoltage event of approx. 0.1 pu occurring at time = 65 seconds. The reactive power decreased from 0 pu down to nearly -0.5 pu following an open-loop response time of 5 seconds. Interestingly, the voltage regulators installed on test site reacted short after the voltage drop concurrently to the Volt-VAR response of the DER. Hence, the jump in the voltage triggered the voltage regulator which brought the voltage back to normal. This has promoted the Volt-VAR function to reduce the reactive power absorption back to -0.05 pu.

Fig. 9 presents the results of Case III, where the Frequency-Watt droop function was tested. The expectation is that when the frequency decrease, active power should increase to provide the active power support to the grid, and vice-versa. To test the functionality, a dip of 0.5 Hz was applied at time = 125 seconds.

The frequency drop provoked an increase in the active power output to 0.95 pu as per the Hz-Watt characteristic with an open-loop response time of 5 seconds. After the frequency recovered, the Freq-Watt function was disabled and consequently the active power supply was reduced back to 0.8 pu.

Note that in Fig. 8 and Fig. 9, apparent plateau behavior appeared on the reactive (90 to 95 sec) and active (125 to 135 sec) power feedback measurements. This plateau behavior was due to spurious transmission delays of the measurement communication protocol caused by the Modbus TCP to Modbus RTU conversion.

Finally, Fig. 10 talks about Case IV, the PV restoration function following an undervoltage trip of the system. The undervoltage event lasted for 20 seconds and the voltage dipped to 0.8 pu. As shown in the figure, the system tripped 4 seconds after the dip, and reconnected 2 seconds after the voltage got to its nominal value. The active power ramped up to its pre-disturbance value shortly after the Enter Service flag switched to true.

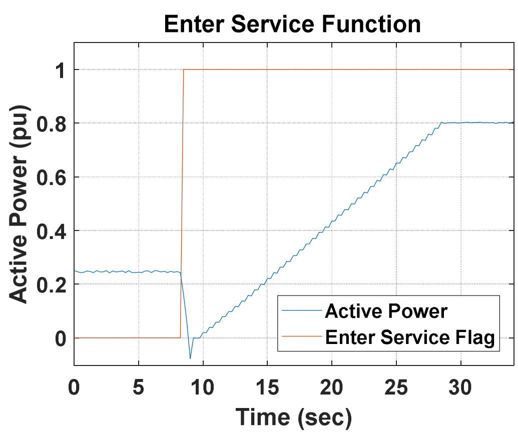


Fig. 7 Case I: BESS Enter Service Activation and Active Power Ramp-Up.

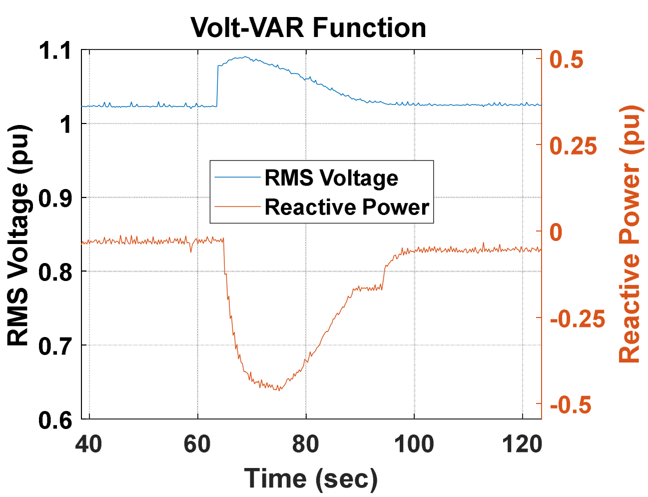


Fig. 8 Case II: BESS Reactive Power Decrease to Over-Voltage, as per Volt-VAR function.

.

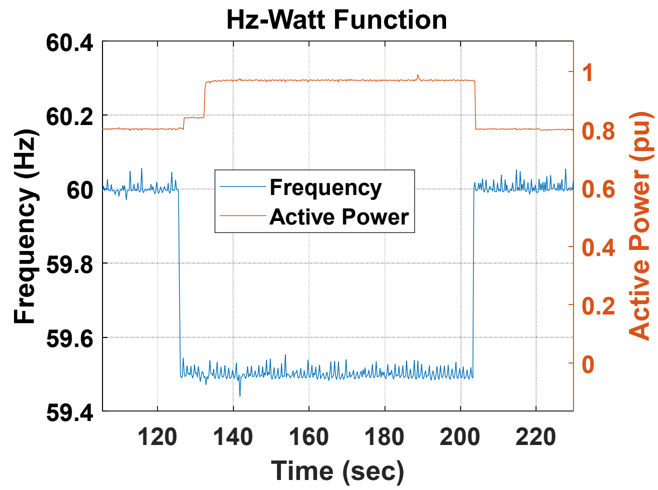


Fig. 9 Case III: BESS Active Power Drop to Over-Frequency, as per Hz-Watt Function.

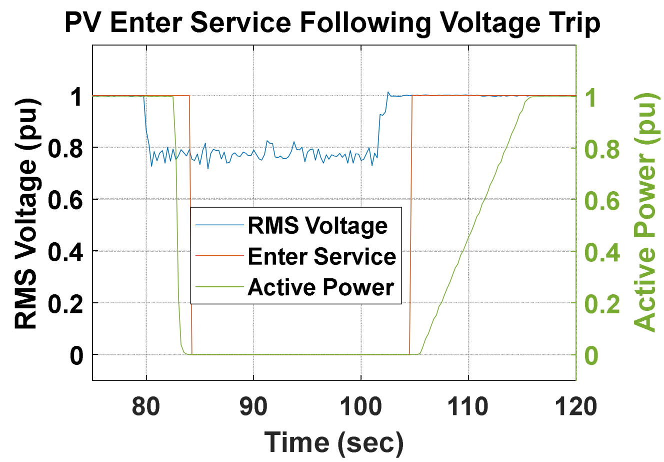


Fig. 10 Case IV: PV Enter Service to Under-Voltage and Restoration.

## IV. Conclusion

In this paper, OpenFMB was utilized to enable distributed intelligence on a grid code controller. The results demonstrate the ability of the grid code controller to subscribe to messages (readings, status) from dissimilar hardware and software vendors and then make distribution level decisions (grid codes) in real time by publishing messages (readings, control and status) and proves the successful Distributed Intelligence operation. The utilized interoperability architecture not only provides access to local coordination and optimization but also supports functioning general local connectivity and local peer-to-peer (publish and subscribe). Using a C-HIL setup, it was demonstrated how it’s possible to enhance existing two DERs, one PV and one BESS, with IEEE 1547-2018 grid code functionalities.

## References


[1] S. Xu, Y. Xue and L. Chang, "Review of Power System Support Functions for Inverter-Based Distributed Energy

Resources- Standards, Control Algorithms, and Trends," *IEEE Open Journal of Power Electronics,* vol. 2, pp. 88-105, 2021.

[2] J. Matevosyan, J. MacDowell, N. Miller, B. Badrzadeh, D. Ramasubramanian, A. Isaacs, R. Quint, E. Quitmann, R. Pfeiffer, H. Urdal, T. Prevost, V. Vittal, D. Woodford, S. H. Huang and J. O'Sullivan, "A Future With Inverter-Based Resources: Finding Strength From Traditional Weakness," *IEEE Power and Energy Magazine,* vol. 19, pp. 18-28, 2021.

[3] "IEEE 1547-2018: IEEE Standard for Interconnection and Interoperability of Distributed Energy Resources with Associated Electric Power Systems Interfaces," IEEE Standards Association, 6th April 2018. [Online]. Available: https://standards.ieee.org/ieee/1547/5915/.

[4] M. Ferrari, A. Sundararajan, N. Shepard, J. Smith and B. Ollis, "Microgrid Communications Using the Open-Source Open Field Message Bus (OpenFMB) Framework Applied to a 480V, 100kW Laboratory Microgrid," in *2022 IEEE 13th International Symposium on Power Electronics for Distributed Generation Systems (PEDG)*, 2022.

[5] "Open Field Message Bus (OpenFMB)," [Online]. Available: https://openfmb.ucaiug.org/Pages/Overview.aspx?#naesb.

[6] "OpenFMB Operational Use Case Data Model," UCA International Users Group, [Online]. Available: https://gitlab.com/openfmb/pim/ops/-/tree/v2.1.0-testing/. [Accessed 4th November 2022].

[7] "North American Energy Standards Borad," [Online]. Available: https://www.naesb.org/. [Accessed 4th November 2022].

[8] "Typhoon HIL604," Typhoon HIL, [Online]. Available: https://www.typhoon-hil.com/doc/products/Typhoon-HIL604-brochure.pdf. [Accessed 4th November 2022].

[9] K. Prabakar, A. Pratt, D. Krishnamurthy and A. Maitra, "Hardware-in-the-Loop Test Bed and Test Methodology for Microgrid Controller Evaluation," in *2018 IEEE/PES Transmission and Distribution Conference and Exposition (T&D)*, Denver, CO, USA, 16-19 April 2018.

[10] F. Mohammadi, R. Bok and M. Hajian, "Real-Time Controller-Hardware-in-the-Loop Testing of Power Electronics Converters," in *2022 13th Power Electronics, Drive Systems, and Technologies Conference (PEDSTC)*, Tehran, Islamic Republic of Iran, 01-03 February 2022.

[11] "PS250 / PS500 Power Conversion System," Hitachi Energy, [Online]. Available: https://search.abb.com/library/Download.aspx?DocumentID=4CAE000834&LanguageCode=en&DocumentPartId=A4-web&Action=Launch. [Accessed 4th November 2022].

[12] "XC modular programmable logic controllers (PLCs)," Eaton Corporation PLC, [Online]. Available: https://www.eaton.com/us/en-us/catalog/machinery-controls/xc-modular-programmable-logic-controllers--plcs-.html. [Accessed 04 November 2022].

[13] "Common Methodologies in Model Based Systems Engineering," Typhoon HIL, 30th September 2022. [Online]. Available: https://www.typhoon-hil.com/methodologies/. [Accessed 4th November 2022].

[14] A. A. Vukojevic, *Design of Reliable and Secure System Protection and Control Schemes in Microgrids Consisting of Inverter-Based Distributed Energy Resources,* Raleigh, NC, USA: North Carolina State University, 2020.

[15] "EPyQ," EPC Power, [Online]. Available: https://github.com/epcpower/st. [Accessed 4th November 2022].